THE JOURNAL OF BIOLOGICAL CHEMISTRY VOL. 291, NO. 6, pp. 3000–3009, February 5, 2016

Regulation of Glucokinase by Intracellular Calcium Levels in Pancreatic β Cells*

Received for publication, September 14, 2015, and in revised form, December 17, 2015 Published, JBC Papers in Press, December 23, 2015, DOI 10.1074/jbc.M115.692160

Michele L. Markwardt, Kendra M. Seckinger[1], and Mark A. Rizzo[2]

From the University of Maryland School of Medicine, Baltimore, Maryland 21201

Glucokinase (GCK) controls the rate of glucose metabolism in pancreatic β cells, and its activity is rate-limiting for insulin secretion. Posttranslational GCK activation can be stimulated through either G protein-coupled receptors or receptor tyrosine kinase signaling pathways, suggesting a common mechanism. Here we show that inhibiting Ca^{2+} release from the endoplasmic reticulum (ER) decouples GCK activation from receptor stimulation. Furthermore, pharmacological release of ER Ca^{2+} stimulates activation of a GCK optical biosensor and potentiates glucose metabolism, implicating rises in cytoplasmic Ca^{2+} as a critical regulatory mechanism. To explore the potential for glucose-stimulated GCK activation, the GCK biosensor was optimized using circularly permuted mCerulean3 proteins. This new sensor sensitively reports activation in response to insulin, glucagon-like peptide 1, and agents that raise cAMP levels. Transient, glucose-stimulated GCK activation was observed in βTC3 and MIN6 cells. An ER-localized channelrhodopsin was used to manipulate the cytoplasmic Ca^{2+} concentration in cells expressing the optimized FRET-GCK sensor. This permitted quantification of the relationship between cytoplasmic Ca^{2+} concentrations and GCK activation. Half-maximal activation of the FRET-GCK sensor was estimated to occur at ~400 nM Ca^{2+}. When expressed in islets, fluctuations in GCK activation were observed in response to glucose, and we estimated that posttranslational activation of GCK enhances glucose metabolism by ~35%. These results suggest a mechanism for integrative control over GCK activation and, therefore, glucose metabolism and insulin secretion through regulation of cytoplasmic Ca^{2+} levels.

Coupling between blood glucose levels and β cell metabolism is achieved first by efficient glucose transport into the β cell and second by the complex enzymatic properties of GCK.[3] Under sufficiently high glucose concentrations *in vitro*, GCK undergoes a conformational shift that accelerates its activity and gives it a non-allosteric sigmoidal dependence for glucose (1). In cells, enhanced GCK activity can be achieved through cysteine *S*-nitrosylation via reaction with NO (2) or by interaction with the phosphofructo-2-kinase/fructose-2,6-bisphosphatase (PFK2) bifunctional enzyme (3, 4). Our laboratory has extensively characterized the regulation of GCK by the NO pathway, describing roles for GCK *S*-nitrosylation in human diabetes (5), incretin hormone signaling (6), and regulation of GCK protein levels (7).

Regulation of GCK by NO proceeds through the neuronal-type NOS (7–9). Prior to activation, GCK associates with NOS dimers on secretory granules (7, 9). *S*-nitrosylation of GCK leads to release of the activated GCK into the cytoplasm. Notably, NO production by this NOS variant requires association with Ca^{2+}-calmodulin (10–12), which completes the electron transport chain and leads to L-arginine catalysis and generation of NO. In islets, NOS activation can dynamically respond to Ca^{2+} oscillations (13), but whether this dynamic behavior can couple to GCK activation is unknown. Furthermore, the nature of the Ca^{2+} signals that lead to GCK activation are unknown. Given that the Ca^{2+} environment in β cells is highly dynamic (14), understanding the precise nature of the signals that lead to GCK activation is important for understanding the physiologic context of GCK regulation. This study employs an optical biosensor approach to quantify the nature of the relationship between cytoplasmic Ca^{2+} levels and GCK activation in living β cells.

We have noted previously that two different signaling systems can stimulate GCK *S*-nitrosylation: insulin (2, 8), which signals through receptor tyrosine kinases and insulin receptor substrate-facilitated pathways (15), and glucagon-like peptide 1 (GLP-1) (6), which signals primarily through G_s protein-coupled receptors (16). Notably, GCK activation can proceed even in the absence of extracellular Ca^{2+} influx or even glucose (8). Given the essential requirement for Ca^{2+} in neuronal NOS activation, we hypothesized that mobilization of the intracellular Ca^{2+} pool, specifically the ER pool, mediates receptor-mediated GCK activation.

Experimental Procedures

Reagents—DNA preparation kits were from Qiagen. DNA primers were from Integrated DNA Technologies. Chemicals were from Sigma-Aldrich unless noted otherwise.

Cell Culture—βTC3 cells (from Ref. 8) and primary islets from 6- to 12-week-old male C57/BL6 mice were cultured and prepared for microscopic observation as described previously (6). All animal care procedures received institutional approval in accordance with federal guidelines. MIN6 cells (from Ref. 17)

* This work was supported by National Institutes of Health Grants R21-DK067415 and R01-DK077140 (to M. A. R.), P60-DK079637, and P30-DK072488. The authors declare that they have no conflicts of interest with the contents of this article. The content is solely the responsibility of the authors and does not necessarily represent the official views of the National Institutes of Health.

[1] Supported by National Institutes of Health Grant T32-GM008181.

[2] To whom correspondence should be addressed: 660 W. Redwood St., HH 525B, Baltimore, MD 21201. Tel.: 410-706-2421; Fax: 410-706-8341; E-mail: mrizzo@som.umaryland.edu.

[3] The abbreviations used are: GCK, glucokinase; ER, endoplasmic reticulum; s, sense; as, antisense; ChR, channelrhodopsin; LED, light-emitting diode; 2-APB, 2-aminoethoxydiphenyl borate; IP_3R, inositol 1,4,5-trisphosphate receptor; CFP, cyan fluorescent protein; ANOVA, analysis of variance.

were cultured in DMEM with 4.5 g/liter glucose, L-glutamine, and sodium pyruvate (Cellgro) supplemented with 10% fetal bovine serum (ThermoFisher); 4 μl/liter β-mercaptoethanol; and 1% penicillin-streptomycin solution (HyClone). INS1E cells (from Ref. 18) were cultured as described previously (18). Transfections were performed using LipoD293 from SignaGen Laboratories according to the instructions of the manufacturer. For fura-2 studies, cells were labeled with 2 μM fura-2 acetoxymethyl ester (40 min, 37 °C) (Invitrogen) prior to washing and experimentation.

Vector Preparation—Circularly permuted mCerulean3 (mCer3) (19) variants were created using the four-primer PCR method, with the GGSGG linker sequences encoded by sense (s) primer 5′-T GGC AGC GGT GGC ATG GTG AGC AAG G-3′ and antisense (as) primer 5′-CC ACC GCT GCC A CC CTT GTA CAG CTC G-3′. These were used in conjunction with the following end primers to generate fragments of the appropriate length: cp49, 5′-TTT A CCG GTC CGC ACC ATG ACC ACC GGC AAG-3′ (s) and 5′-CCC AGA TCT GAG TCC GGA GCA GAT GAA CTT CAG GG-3′ (as); cp157, 5′-TTTA CCG GTC CGC ACC ATG CAG AAG AAC GGC-3′ (s) and 5′-CCC AGA TCT GAG TCC GGA CTT GTC GGC GGT-3 (as); cp173, 5′-TTT ACC GGT CGC CAC CAT GGA CGG CAG CGT G-3′ (s) and 5′-CCC AGA TCT GAG TCC GGA CTC GAT GTT GCA GTT GC-3′ (as); cp195, 5′-TTT A CCG GTC CGC ACC ATG CTG CCC GAC AA-3′ (s) and 5′-CCC AGA TCT GAG TCC GGA CAG CAC GGG GC-3′ (as). N- and C-terminal fragments were linked and amplified by PCR prior to insertion into derivative pQE9 and C1 vectors using AgeI and BglII restriction sites (20). Subsequent cloning into FRET-GCK (8) from C1 vectors was accomplished using NheI and BglII restriction sites. The sequences were confirmed by DNA sequencing (Genewiz). Generation of recombinant proteins and spectroscopic characterization were performed as described previously (19). The ER-localized channelrhodopsin (ChR)-mCherry-ER construct was created by fusing the ER retention sequence from pER-ECFP (Clontech) to the C terminus of hChR2(H134R-mCherry (21) using BsrGI and XbaI restriction sites.

Adenoviral vectors were constructed by subcloning the FRET-GCK biosensor coding sequence into an existing pAdTrack-CMV vector. Viruses were then generated by the Mid-Atlantic Nutrition Obesity Research Center core facility using the AdEasy system (22).

Fluorescence Microscopy—FRET imaging and NADH/NADPH (collectively referred to as NAD(P)H) autofluorescence assays were performed using confocal/two-photon microscopy (5) or wide-field microscopy (6) methods as indicated and as described previously. Imaging devices, conditions, and the imaging buffer have been described in detail elsewhere (5, 6). Specimens for Fluo-4 imaging were prepared by labeling cells with acetoxymethyl ester conjugate (Life Technologies, 5 μM, 30 min, 37 °C) according to the recommendations of the manufacturer. Data were collected in the wide field under 470-nm LED illumination and a high-efficiency enhanced GFP filter cube (Zeiss) for collection.

Quantitative fura-2/FRET imaging was performed essentially as described previously (23) but incorporated 360- and 380-nm LED illumination for collecting fura-2 fluorescence. Ca^{2+} concentrations were obtained using the fura-2 Ca^{2+} imaging calibration kit (Invitrogen) according to the kit instructions. For experiments utilizing ChR-mCherry-ER, FRET biosensor illumination was changed to 400 nm, whereas 455-nm pulses were used to activate ChR. ChR-mCherry-ER fluorescence was captured using 530-nm LED illumination with the Zeiss dsRed (no. 43) filter set prior to experimentation. ChR was activated by manual triggering of 455-nm LED fluorescence for ~1-s intervals as indicated, except for collection of quantitative data for curve fitting. For those experiments, the Zeiss AxioVison Smart Experiments function was used to precisely activate ChR using three trains of 15 1-s pulses. FRET ratios from maximum cytoplasmic [Ca^{2+}] obtained before and after pulsing were normalized to FRET ratios obtained from mutant GCK proteins resistant to *S*-nitrosylation (5, 8). Cross-talk fluorescence was subtracted from FRET signals as described previously (23). The minimum FRET-GCK ratio was approximated from using a sensor containing the C371S mutation (FRET ratio, 0.27 $\pm$ 0.009 (S.E.), $n = 10$ independent replicates). The maximum FRET ratio was estimated by treatment of cells expressing the FRET-GCK with 100 μM diethylamine NONOate (Calbiochem) (FRET ratio, 0.42 $\pm$ 0.015, $n = 15$ independent replicates). Curve fitting and statistical analysis was performed using GraphPad Prism software. Image analysis was performed using Zeiss Axiovision software or ImageJ. The non-ratio images in Figs. 3*F*, 3*G*, and 4*B* were pseudocolored cyan and yellow using Adobe Photoshop. Ratio images were generated from the original images by using ImageJ software for smoothing, image ratioing, masking the background, and applying the pseudo-color look-up table. ImageJ was also used to generate the kymograph in Fig. 4*B*.

Results

ER Ca^{2+} Couples Receptor Signaling to GCK Activation—To study dynamic GCK regulation, we utilized two methods we established previously as useful assays for studying GCK activation by NO in living cells. First, we developed a FRET-GCK biosensor on the basis of the GCK structure that can sensitively report activation by *S*-nitrosylation (8, 24). Second, we can quantify glucose-stimulated changes in NAD(P)H autofluorescence (5–7). Because GCK is rate-limiting for glucose metabolism (25), changes in GCK activity are reflected by glucose-dependent rises in NAD(P)H (26). Therefore, stimulation of GCK *S*-nitrosylation results in corresponding potentiation of glucose-stimulated rises in NAD(P)H autofluorescence (5). These previously established assays were used to probe the relationship between changes in cytoplasmic Ca^{2+} and GCK activation.

To test whether insulin-stimulated FRET-GCK biosensor activation requires Ca^{2+} release from the ER, we used inhibitors of the two primary ER Ca^{2+} channels: 2-aminoethoxydiphenyl borate (2-APB) (27) to block inositol 1,4,5-trisphosphate receptors (IP_3Rs) and inhibitory concentrations of ryanodine (28, 29) to block Ca^{2+} release from ryanodine receptors (Fig. 1*A*). Both of these agents inhibited activation of FRET-GCK by insulin. Furthermore, stimulating concentrations of ryanodine (2.5 nM) also activated the FRET-GCK sensor, indicating that inducing ER-Ca^{2+} release is sufficient for activating GCK. Importantly, these inhibitors did not signifi-

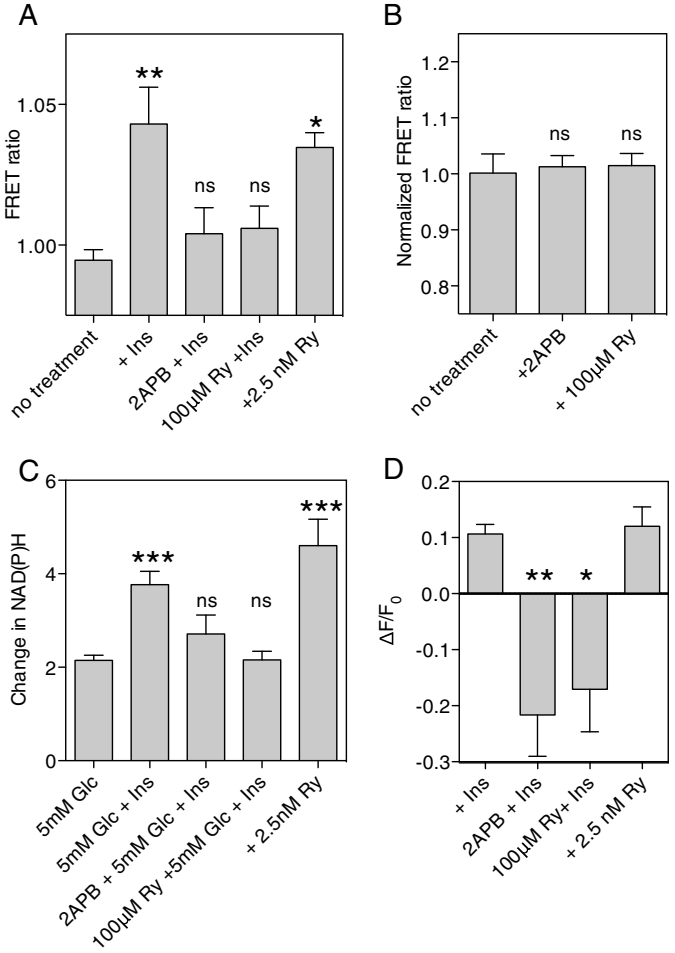

FIGURE 1. **Insulin-stimulated activation of GCK requires release of ER Ca^{2+}.** *A*, βTC3 cells expressing the FRET-GCK sensor were glucose-starved for 3 h prior to treatment as indicated. Cells were observed by fluorescence microscopy, and FRET ratios were normalized to baseline conditions as described previously (6). Treatment was with 100 nM insulin (*Ins*, 5 min) or a stimulatory dose of ryanodine (*Ry*, 2.5 nM). Inhibitors of IP_3Rs (100 μM 2-APB) and ryandonine receptors (100 μM ryanodine) were applied prior to stimulation. *Error bars* indicate mean ± S.E. ($n \geq 5$ independent replicates). **, $p < 0.01$; *, $p < 0.05$; *ns*, not significant as determined by ANOVA. *B*, FRET ratios from βTC3 cells expressing the FRET-GCK sensors and left untreated or treated with 100 μM 2-APB or 100 μM ryanodine. The ratios were normalized to the untreated group. ANOVA was used to determine statistical significance. *ns*, $p > 0.05$ compared with the untreated group, Tukey's multiple comparison test, $n = 5$ independent replicates; *error bars* indicate mean ± S.E. *C*, -fold increase in NAD(P)H autofluorescence was measured by two-photon microscopy of cultured βTC3 cells as described previously (5). Treatments were as in *A*, with the inclusion of 5 mM glucose (*Glc*) with the stimulatory dose. Results were normalized to pretreatment NAD(P)H fluorescence ($n \geq 15$ independent replicates). ***, $p < 0.001$ by ANOVA; *ns,* not significant as determined by ANOVA. *D*, effects of the selected treatments on intracellular Ca^{2+} in cells labeled with Fluo-4 ($n = 5$ independent replicates). *, $p < 0.05$; **, $p < 0.01$ by ANOVA compared with the insulin-treated group; *error bars* indicate mean ± S.E.). Change in fluorescence was normalized to baseline ($\Delta F/F_0$).

cantly affect the basal FRET ratio (Fig. 1*B*). Similarly, potentiation of glucose metabolism by insulin, as measured by increased NAD(P)H autofluorescence, was inhibited by application of ER Ca^{2+} channel blockers (Fig. 1*C*), supporting a role for ER Ca^{2+} in activating GCK. Consistent with our FRET-GCK experiment, the activating dosage of ryanodine (2.5 nM) also potentiated glucose metabolism (Fig. 1*C*). The effects of the treatments on cytoplasmic Ca^{2+} were confirmed in cells labeled with Fluo-4 (Fig. 1*D*). Co-stimulation with insulin and ER Ca^{2+} channel blockers significantly decreased cytoplasmic Ca^{2+} levels through mechanisms that are not entirely clear but may be related to direct association of phosphorylated IRS proteins with sarcoendoplasmic reticulum calcium transport ATPase Ca^{2+} pumps on the ER (30).

We next tested whether ER Ca^{2+} release is a general mechanism for GCK activation by testing whether GLP-1, a G protein-coupled receptor agonist, also requires ER Ca^{2+} to activate GCK. Inhibition of ER Ca^{2+} release blocked activation of the FRET-GCK biosensor (Fig. 2*A*), potentiation of glucose metabolism (Fig. 2*B*), and GLP-1-stimulated increases in cytoplasmic Ca^{2+} (Fig. 2*C*). These findings are consistent with the required mobilization of the ER Ca^{2+} pool for GCK activation. Therefore, release of ER Ca^{2+} appears to be an important regulator of GCK activity and glucose metabolism in β cells.

Glucose Stimulates GCK Activation—Our observations raise the important question of whether glucose itself can regulate GCK through the *S*-nitrosylation mechanism. Although receptor signaling is known to enhance Ca^{2+}-induced Ca^{2+} release from intracellular stores (31–35), Ca^{2+}-induced Ca^{2+} release can be observed in the absence of receptor-mediated signaling (36, 37), albeit to a lesser extent. Although we did not find conclusive evidence supporting glucose-specific regulation of GCK in our initial studies (8), our earliest-generation FRET-GCK biosensors were hampered by incorporating fluorescent proteins with low brightness and unstable fluorescence (19) and may have missed smaller glucose effects because of the poor signal-to-noise ratio of the biosensor.

An optimized FRET-GCK sensor with improved brightness and sensitivity was developed by incorporating circularly permuted cyan fluorescent proteins (CFPs) derived from mCer3 (19). These new CFPs were created by linking the natural N and C termini of mCer3 by a GGSGG linker. New N termini were created at amino acid positions 49, 157, and 195 (Fig. 3*A*). Each new mCer3 variant was substituted into the FRET donor position in the FRET-GCK sensor and expressed in βTC3 cells. Cells were stimulated with GLP-1 to activate the sensor, and the increase in FRET ratio, or dynamic range, was normalized to the standard deviation of FRET ratios in unstimulated cells (Fig. 3*B*). The optimized FRET-GCK sensor containing cp173-mCer3 provided contrast over 10 S.D. and was the FRET-GCK sensor used for the rest of this study. The variant incorporating cp157-mCer3 was also bright and outperformed the previous-generation sensor, leading us to further characterize the fluorescence properties of this protein in addition to cp173-mCer3. The excitation and emission spectra of cp157-mCer3 (ϵ, 25000 $M^{-1}cm^{-1}$; quantum yield, 0.77) and cp173-mCer3 (ϵ, 25000 $M^{-1}cm^{-1}$; quantum yield, 0.86) were comparable with the parent mCer3 protein (Fig. 3, *C–E*). Furthermore, we examined the subcellular distribution of the optimized FRET-GCK sensor containing cp173-mCer3. Stimulation with GLP-1 (Fig. 3*F*) or 2.5 nM ryanodine (Fig. 3*G*) resulted in similar activation patterns as those observed using earlier versions of the FRET-GCK sensor (8, 24) and is consistent with activation on secretory granules and translocation to the cytoplasm (2, 7).

To further explore the conditions underlying the molecular regulation of the FRET-GCK sensor, we tested the effect of glucose fasting conditions (8) on the regulation of GCK by

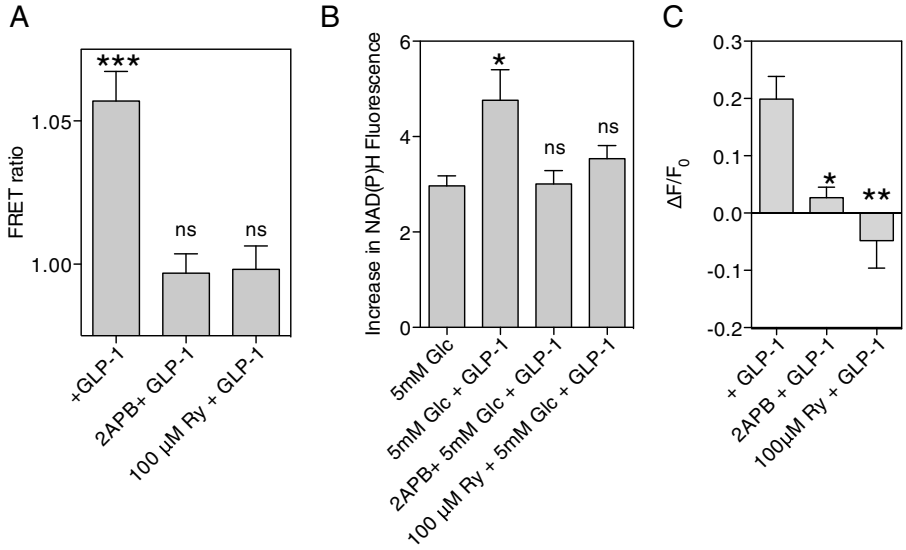

FIGURE 2. **GLP-1-stimulated activation of GCK requires release of ER Ca^{2+}.** *A*, βTC3 cells expressing the FRET-GCK sensor were glucose-starved for 3 h prior to treatment as indicated. Cells were observed by fluorescence microscopy, and FRET ratios were normalized to baseline conditions. Treatment was with 30 nM GLP-1 (5 min). Inhibitors of IP_3Rs (100 μM 2-APB) and ryandonine receptors (100 μM ryanodine) were applied prior to stimulation. *Error bars* indicate mean ± S.E. $n \geq 6$ independent replicates. ***, $p < 0.001$ by ANOVA; *ns,* not significant as determined by ANOVA. *B*, -fold increase in NAD(P)H autofluorescence was measured by wide-field microscopy of cultured βTC3 cells as described previously (7). Treatments were as in *A*, with the inclusion of 5 mM glucose with the stimulatory dose. Results were normalized to pretreatment NAD(P)H fluorescence. $n \geq 10$ independent replicates; *, $p < 0.05$ by ANOVA; *ns,* not significant as determined by ANOVA). *C*, effects of the selected treatments on intracellular Ca^{2+} in cells labeled with Fluo-4 ($n = 5$ independent replicates; *, $p < 0.05$; **, $p < 0.01$ by ANOVA; *error bars* indicate mean ± S.E. Change in fluorescence was normalized to baseline ($\Delta F/F_0$).

GLP-1 and insulin (Fig. 3*H*). Our previous studies have noted that a brief glucose starvation period does not adversely affect βTC3 cells (6), but it is unclear whether stimulation of FRET-GCK could occur in cells exposed to low amounts of glucose that do not elicit secretion. Changing the glucose fasting conditions to 2 mM did not significantly affect the ability of GLP-1 or insulin to stimulate GCK activation (Fig. 3*H*). Further analysis by two-factor ANOVA ($p > 0.05$) did not show significant interaction between basal glucose conditions and stimulation. Prestimulated FRET ratios for low-glucose and glucose-free conditions were not significantly different ($p > 0.05$, ANOVA, Tukey multiple comparison test). We also found that increasing cAMP levels with forskolin or isobutylmethylxanthine activated the FRET-GCK sensor (Fig. 3*I*), consistent with previous work tying cAMP levels to GLP-1 activation of GCK (38). The ability of these treatments to affect cAMP levels in βTC3 cells was confirmed in cells expressing the ICUE3 cAMP FRET indicator (39) (Fig. 3*J*).

Fluctuations in FRET-GCK activation patterns (Fig. 4, *A* and *B*) were observed in the presence of 5 mM glucose. Representative traces are shown in Fig. 4*A* (*red* and *blue*), and the FRET ratio increases over time compared with cells left unstimulated (*black*). Coincident changes to FRET-GCK activation and Ca^{2+} were observed in response to glucose (Fig. 4*C*) in cells labeled with fura-2 to track Ca^{2+} changes (23). Even so, the FRET-GCK ratio decreased rapidly, likely from diffusion out of the region of interest. This is supported by our previous work on the compartmentalized nature of GCK regulation and by the low magnitude of the FRET ratio change. By 3 min, glucose-activated FRET decreases to ~50% of the levels observed for stimulation through cell surface receptors or manipulators of cAMP (Fig. 3, *H* and *I*).

The relatively weak stimulation of GCK by glucose may be related to the βTC3 cell model, which shows key differences from islets with respect to their glucose-stimulated Ca^{2+} behaviors. Notably, they lack the ability to oscillate and are known for their highly variable response to glucose (33). MIN6 cells, however, are known to exhibit oscillatory Ca^{2+} behaviors (17, 40–42) similar to those reported in islets. To investigate potential regulation of GCK by Ca^{2+} oscillations, MIN6 cells expressing the optimized FRET-GCK sensor were labeled with fura-2. Under low-glucose conditions (2 mM, Fig. 5), Ca^{2+} remained low, and no changes in GCK biosensor FRET were observed. Increasing glucose levels to 20 mM in the presence of tetraethylammonium (41, 43) induced Ca^{2+} oscillations (Fig. 5*A*). Strong activation of FRET-GCK was observed only in response to the initial Ca^{2+} influx. The response persisted for several minutes with a slow deactivation. The response is likely maximal because the sensor did not respond to later Ca^{2+} oscillations. Physiologic glucose levels (7.5 mM) also produced similar results, although with dissimilar patterns of Ca^{2+} oscillations (Fig. 5, *B* and *C*).

Optical Release of ER Ca^{2+} Can Activate GCK—To quantify the relationship between cytoplasmic Ca^{2+} concentration and GCK activation more systematically, we developed an approach to optically stimulate release of Ca^{2+} from the ER. However, resting Ca^{2+} levels at 2 mM glucose in βTC3 cells and MIN6 cells (Fig. 6*A*) proved to be highly variable and poorly suited to such an approach. A third cell line, INS1E cells, displayed consistently low levels of intracellular Ca^{2+}, making it most suitable for quantifying the relationship between intracellular Ca^{2+} levels and GCK activation using an optically gated cation channel. An mCherry-tagged channelrhodopsin was targeted to the ER (ChR-mCherry-ER) (Fig. 6*B*). ChRs are non-selective cation

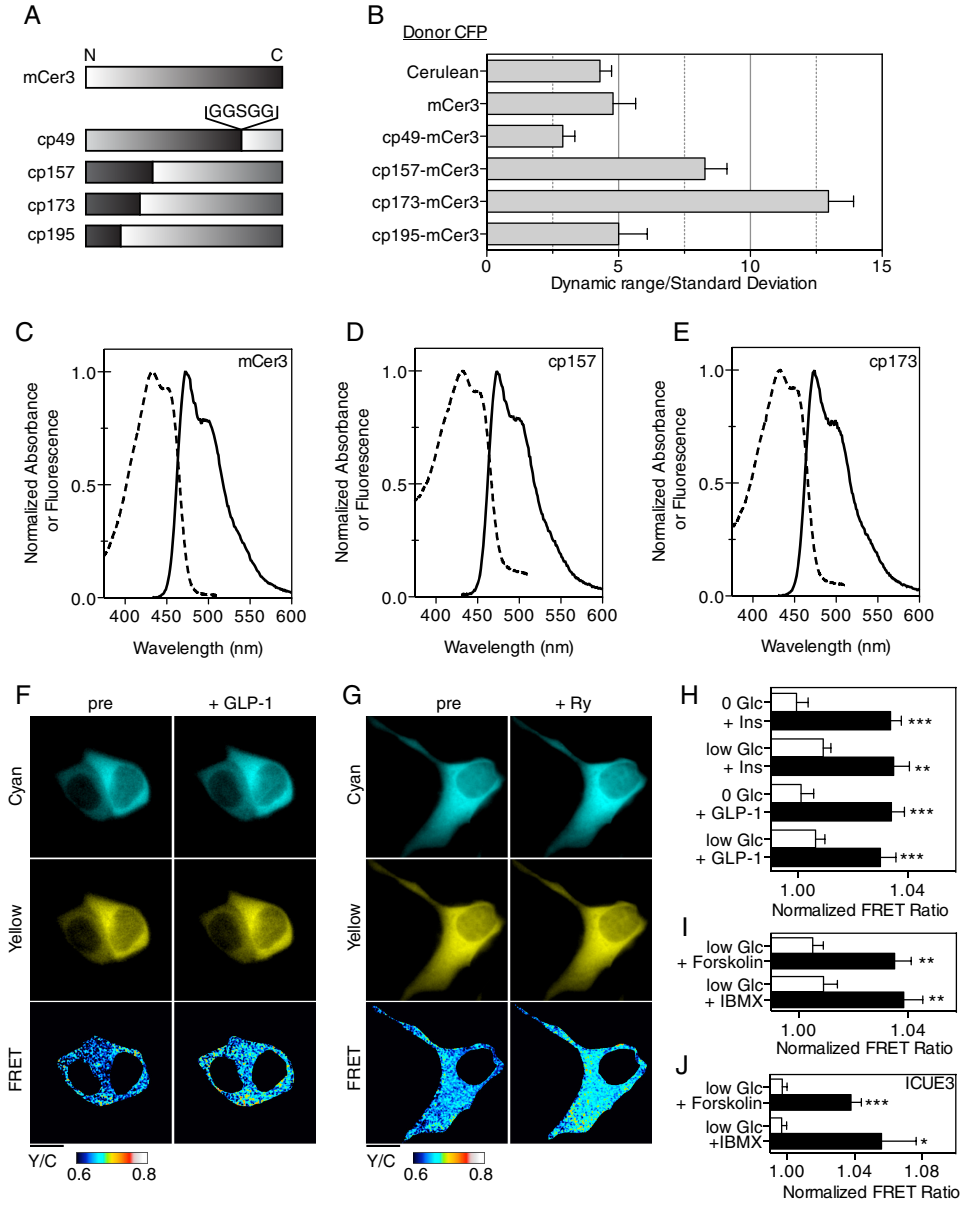

FIGURE 3. **Creation of an optimized FRET-GCK sensor.** *A*, circularly permuted versions of mCer3 were created by linking the N and C termini with a GGSGG linker. New starting codons were inserted at several positions in the mCer3 sequence as indicated. *B*, FRET-GCK sensors were created using these new circularly permuted mCer3 variants, and the baseline FRET ratio was measured in glucose-starved βTC3 cells. Cells were treated with GLP-1 (30 nM, 3 min) to quantify the dynamic range ($n \geq 5$ independent replicates, *error bars* indicate S.E.). *C–E*, absorption (*dashed lines*) and emission spectra (*solid lines*) of cp157-mCer3 and cp173-mCer3 variants were comparable with the parent protein in purified protein samples. *F* and *G*, activation of the optimized FRET-GCK sensor containing cp173-mCer3 in βTC3 cells observed in response to treatment with GLP-1 (*F*, 30 nM, 3 min) or ryanodine (*G*, *Ry*, 2.5 nM, 3 min). The images were collected under CFP-specific, wide-field illumination, and uncorrected ratio images were made by dividing the two images. FRET images were pseudocolored to represent the indicated FRET range (*Y/C*, yellow/cyan fluorescence). *Scale bars* = 10 μm. Non-cytoplasmic regions were masked in the ratio (FRET) image for clarity. *H–J*, βTC3 cells expressing the FRET-GCK sensor (*H* and *I*) or ICUE3 cAMP sensor (*J*) were incubated under glucose-free or low-glucose (*Glc*) conditions (2 mM) for 3 h prior to stimulation with 30 nM GLP-1 (*H*), 100 nM insulin (*Ins*, *H*), 5 μM forskolin (*I* and *J*), or 100 μM isobutylmethylxanthine (*IBMX*, *I* and *J*) as indicated. FRET measurements are shown for time points preceding stimulation (*white columns*) and 3 min post-stimulation (*black columns*). Values were normalized to the baseline, and *error bars* indicate S.E. ($n = 7$ independent replicates for FRET-GCK and 5 independent replicates for ICUE3; *, $p < 0.05$; **, $p < 0.01$; ***, $p < 0.001$; paired *t* test for individual treatments).

channels that can be activated optically (44, 45). Insertion of an ER retention sequence into the C terminus of the mCherry epitope tag constrained its localization to the ER, as evidenced by colocalization with a luminal ER Ca^{2+} sensor (Fig. 6*B*). Using optical pulses, we were able to recreate similar changes in cytoplasmic Ca^{2+} in cultured β cells, as observed naturally (Fig. 6*C*). Furthermore, when co-expressed with an ER-localized FRET Ca^{2+} sensor (D1) (46), optical stimulation of ChR-mCherry-ER resulted in depletion of Ca^{2+} from the ER, as indicated by a change in the FRET ratio (Fig. 6*D*). Prolonged elevation of the cytoplasmic Ca^{2+} concentration was achieved by manipulation of pulsing conditions (Fig. 6*E*). This permitted quantification of the relationship between the cytoplasmic Ca^{2+} concentration and GCK biosensor activation (Fig. 6*F*). Half maximal activation of the biosensor was observed at ~400 nM Ca^{2+}, with a steep Hill coefficient in the 4–6 range (95% confidence intervals). These values

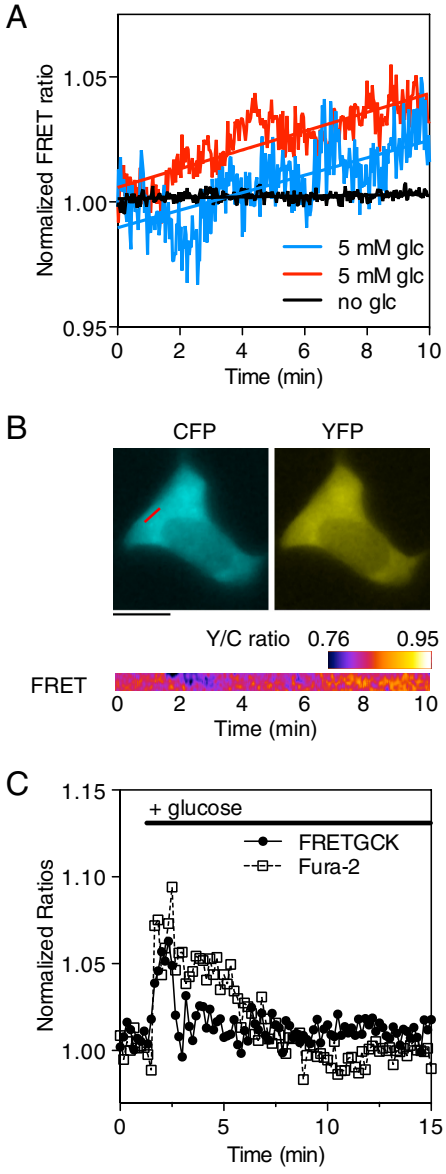

FIGURE 4. **Glucose stimulates periodic activation of GCK in βTC3 cells.** *A*, fluctuating FRET (YFP/CFP) ratios in βTC3 cells were observed in the presence of 5 mM glucose (*glc*, *blue* and *red*) but not under glucose-free conditions (*black*). FRET ratios were normalized to the initial intensity values. *Lines* indicate linear regression to show overall trend. *B*, CFP and YFP images under CFP illumination for a cell incubated with 5 mM glucose. *Bottom panel*, kymograph of FRET ratio images for the region indicated by the *red line* (*CFP panel*). FRET ratios (*Y/C*, yellow/cyan fluorescence) are represented by the indicated colors. *Scale bar* = 10 μm. *C*, βTC3 cells were transfected with the sensor and labeled with fura-2 for quantification of Ca^{2+}. Glucose stimulation resulted in increased Ca^{2+} and FRET-GCK sensor activation.

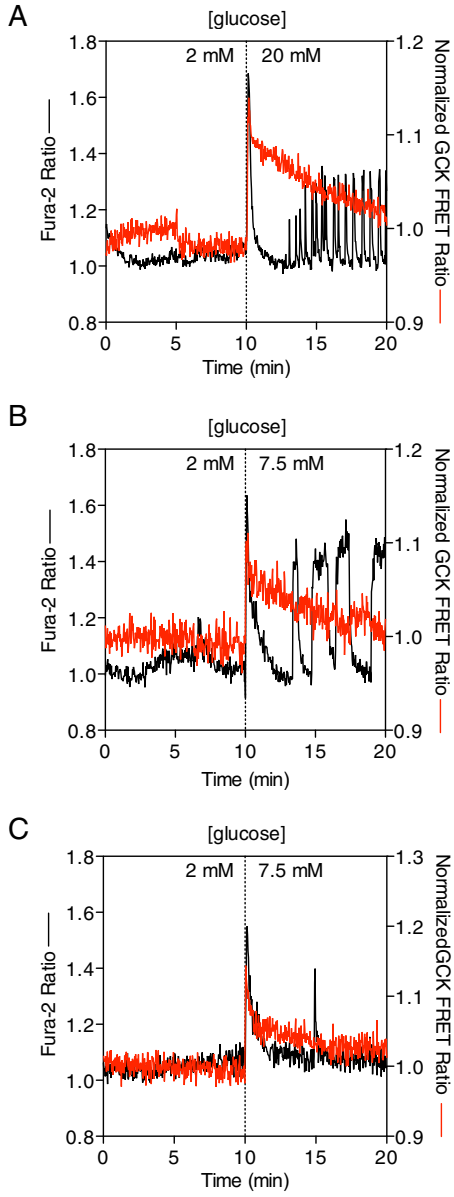

FIGURE 5. **GCK activation in MIN6 cells during Ca^{2+} oscillations.** *A*—*C*, MIN6 cells expressing the optimized FRET-GCK sensor were labeled with fura-2. Cells were incubated in 2 mM glucose prior to stimulation with high glucose (20 mM total, *A*) or physiologic glucose (7.5 mM total, *B* and *C*) and 20 mM tetraethylammonium to stimulate Ca^{2+} oscillations, as indicated by the *dashed line*. Fura-2 ratios are represented by the *black traces*, and FRET ratios normalized to the mean 2 mM ratio are colored *red*. FRET-GCK activation was associated with the initial Ca^{2+} influx but not subsequent rises in Ca^{2+} for fast (*A*), slow (*B*), or stochastic (*C*) patterns of Ca^{2+} oscillations.

agree well with the measured half-maximal activity of NOS *in vitro* (~300 nM) (47) and the proposed stoichiometry of Ca^{2+}-calmodulin-mediated activation of dimeric NOS (12, 48).

To explore whether glucose can activate GCK in a more physiologic context, the optimized FRET-GCK biosensor was expressed in primary mouse islets. Fluctuations in sensor activation were observed under continuous glucose stimulation (Fig. 7*A*) or upon transition from 2 to 7.5 mM glucose stimulation (Fig. 7*B*). Fluctuations in GCK activation were observed in parallel with fluctuations in NAD(P)H fluorescence (Fig. 7*B*). Furthermore, glucose failed to activate two mutant sensors that are not *S*-nitrosylated (Fig. 7*C*, *white*). Glucose-stimulated changes in NAD(P)H were also reduced in the cells expressing theses mutant sensors (Fig. 7*C*, *white*) even though these mutations do not substantially alter glucose phosphorylation kinetics *in vitro* (2, 5). These results suggest that the glucose-stimulated GCK *S*-nitrosylation potentiates metabolism by an additional ~35%.

Discussion

The Optimized FRET-GCK Sensor and ChR-ER Are Enabling Technical Advances—Here we developed two novel reagents that enable a more sensitive study of the regulation mecha-

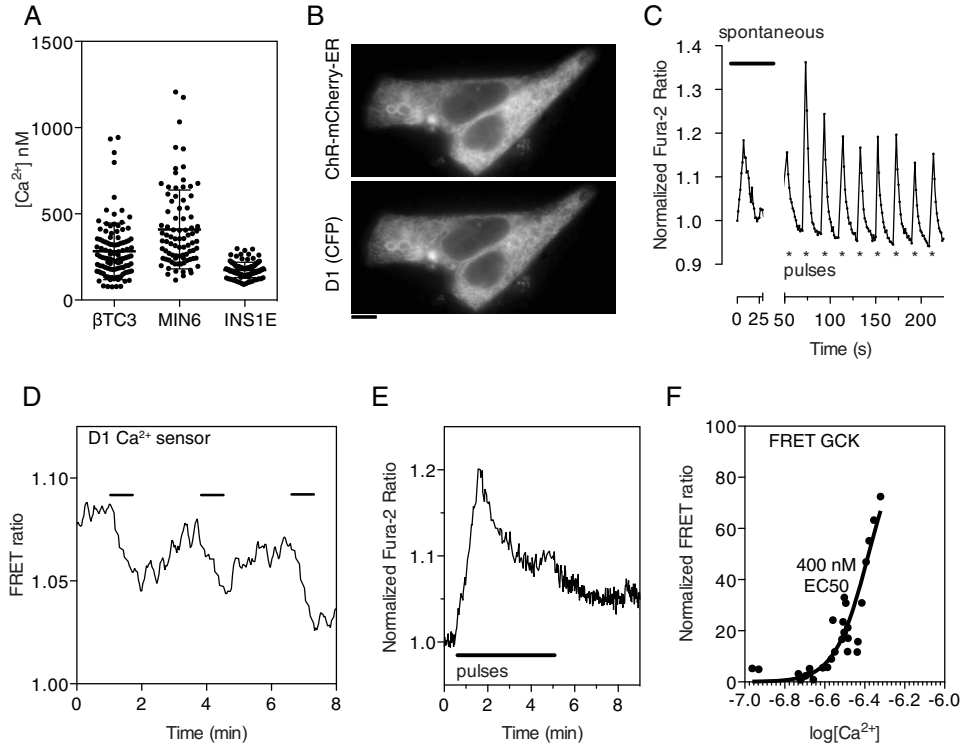

FIGURE 6. **Use of ChR to characterize the relationship between GCK activation and cytoplasmic Ca^{2+}.** *A*, resting levels of Ca^{2+} for βTC3, MIN6, and INS1E cells in 2 mM glucose as measured using fura-2 ($n > 80$ independent replicates). INS1E cells display consistently low Ca^{2+} levels that enable systemic study of the Ca^{2+}/GCK relationship using an ER-localized ChR. *B*, co-expression of ER-localized ChR-mCherry-ER and an ER-localized Ca^{2+} indicator in INS1E cells. *Scale bar* = 10 μm; a cyan fluorescent protein image is shown for the D1 sensor. *C*, spontaneous and optically induced Ca^{2+} behaviors were tracked in INS1E cells expressing ChR-mCherry-ER and labeled with fura-2. The *asterisks* indicate pulses of 455-nm LED light (1 s). *D*, INS1E cells co-expressing ChR-mCherry-ER and the D1 FRET-based Ca^{2+} sensor were exposed to activated light pulses (indicated by *bars*). Depletion of the ER-Ca^{2+} is indicated by a decrease in the FRET ratio. Data were smoothed for presentation clarity (GraphPad Prism, second-order smoothing). *E*, closely spaced pulses were used to raise the cytoplasmic Ca^{2+} concentration of an INS1E cell expressing ChR-mCherry-ER. *F*, fura-2 was used to quantify the cytoplasmic Ca^{2+} concentration in cells expressing ChR-mCherry-ER and the FRET-GCK biosensor. Optical pulses were used to raise cytoplasmic Ca^{2+} concentration, and FRET-GCK activation was normalized as described under "Experimental Procedures." Data were fit using a log(agonist) *versus* normalized response model.

nisms that control β cell glucose metabolism. Creation of the circularly permuted mCer3 variants provided an efficient method for sensor optimization. Simple swapping of mCerulean for the brighter mCer3 did improve the brightness of the probe but not its performance in this case, as defined by improvement of the ratio of the dynamic range to measurement precision. This is consistent with our experience with upgrading the first generation ECFP to Cerulean, where the dynamic range between activated and deactivated FRET conformations was decreased slightly (24). Notably, circular permutation of mCer3 was well tolerated, and the optimized FRET-GCK sensor containing cp173-mCer3 displays greatly improved contrast between *S*-nitrosylated and denitrosylated conformations while retaining the advances in measurement precision associated with mCer3 development (19).

To our knowledge, this is the first use of an optically gated, non-selective cation channel to stimulate release of Ca^{2+} from the ER. ChR-mCherry-ER was useful for systematic exploration of the relationship between GCK activation and ER Ca^{2+} release. Unlike permeabilized cell approaches, the integrity of the cytoplasmic environment remains intact. Here we show that periodic Ca^{2+} oscillations can be recreated in culture. Therefore, we expect that this approach will be useful for exploring the function of Ca^{2+} oscillations not only for β cell physiology but for other systems where oscillatory activity is known to occur (49). Even so, our approach has special utility for studying β cells and should permit close examination of the spatial aspects of GCK regulation (50, 51) and enable a more direct exploration of the connection between metabolic and Ca^{2+} oscillations in living β cells. Finally, the optical approach for modulating ER Ca^{2+} offers advantages over pharmacological agents, like 2-APB, that have off-target effects and complex pharmacology (52).

Cytoplasmic Ca^{2+} and GCK Activation—Our data suggest a tight connection between a rise in the cytoplasmic Ca^{2+} concentration and GCK activation. The initial Ca^{2+} influx following exposure to stimulatory concentrations of glucose seems to be most important and, in islets and MIN6 cells, leads to a prolonged activation of GCK spanning several minutes. Even in βTC3 cells, low levels of activated GCK tended to rise over time, fitting well with what is known about the mechanism of GCK activation. Association with NOS on secretory granules is essential for GCK activation (7) and results in dissociation of the complex and release of GCK into the cytoplasm. The mechanism behind denitrosylation of GCK is unknown but does not appear to be rapid enough to allow fast cycling of GCK activation. Rather, the model we favor is a burst of GCK activation following exposure to post-prandial conditions (*i.e.* high glucose and hormones such as GLP-1), perhaps contributing to the first phase of insulin secretion or the highly dynamic first

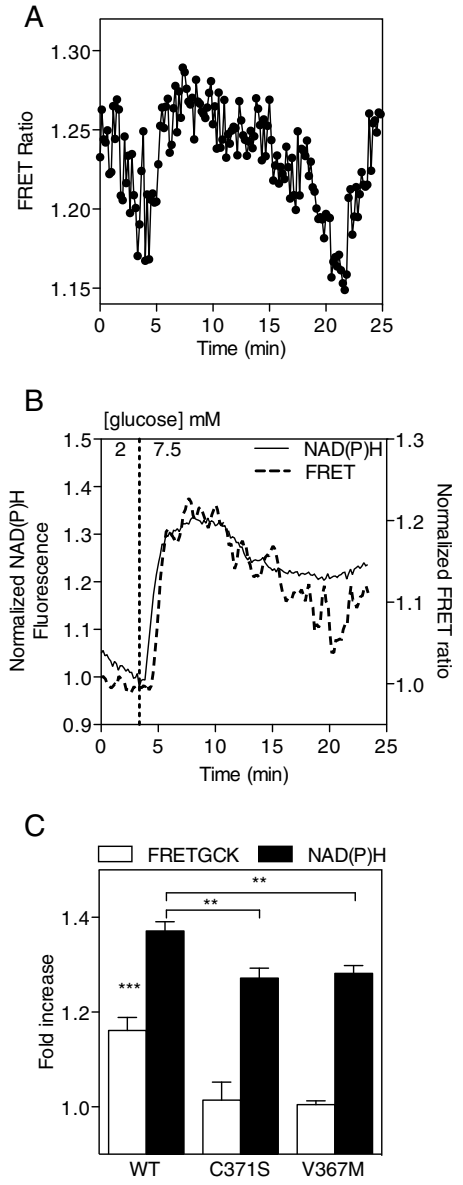

FIGURE 7. **Glucose-stimulated regulation of GCK in islets.** *A*, the optimized FRET-GCK sensor was expressed in an isolated mouse islet using adenoviral vectors. Dynamic changes in the FRET ratio were observed by fluorescence microscopy in an islet stimulated with 7.5 mM glucose. *B*, FRET-GCK activation was tracked along with changes in NAD(P)H fluorescence in an islet cell stimulated with 7.5 mM glucose (total). The change from 2 to 7.5 mM glucose is indicated by the *dashed line*. Normalization was to resting (2 mM glucose) values. *C*, islet cells expressing WT sensors or those with mutations that block GCK *S*-nitrosylation (V367M and C371S). FRET ratios and NAD(P)H autofluorescence were measured by fluorescence microscopy before (2 mM glucose) and after addition of glucose (7.5 mM total). *Error bars* indicate mean ± S.E. $n \geq 9$ independent replicates; **, $p < 0.01$; ***, $p < 0.001$; ANOVA.

responder type of secretion observed *in vivo* (53), although that remains to be proven.

Also unclear is the relationship between glucose and hormonal activation of GCK. Strong stimuli, such as those used to induce GCK oscillations in MIN6 cells, seem to saturate GCK activation, whereas stimulation of islets with physiologic levels of glucose does seem to allow the possibility of low-frequency GCK oscillations. The actual physiology underlying hormone stimulation of islet function is not well understood because it is difficult to distinguish between systemic and direct actions of hormones such as insulin (54), GLP-1 (55), and kisspeptin (56, 57). Synergistic GCK activation between glucose and hormonal signaling can occur at multiple levels, especially those influencing cAMP dynamics (58), as suggested by our finding that increasing cAMP levels with forskolin or isobutylmethylxanthine can activate GCK. A detailed investigation will be required to understand the nuances of GCK regulation during co-stimulation.

With regards to the dependence of GCK on ER Ca^{2+} *versus* Ca^{2+} influx, our pharmacological studies strongly support a role for ER Ca^{2+}, but, as noted above, interpretation of these studies can be difficult because such agents tend to be less specific than desired. Even so, it is questionable whether extracellular Ca^{2+} influx during an action potential would raise cytoplasmic Ca^{2+} levels high enough to activate GCK. Previous measurements have found that extracellular Ca^{2+} is buffered quickly and raises Ca^{2+} levels only within a short distance from the plasma membrane (59). Furthermore, we have shown that extracellular Ca^{2+} influx is not essential for activating GCK because it can be observed in the presence of voltage-gated Ca^{2+} channel blockers (8). Taken together with our finding that activation of our GCK sensor by ER-ChR requires raising cytoplasmic Ca^{2+} to ~300–400 nM, GCK activation almost certainly requires mobilization of the ER Ca^{2+} pool. The proposed ER-Ca^{2+} mechanism also makes sense from the vantage point of spatial regulation of GCK activation, given that release of ER Ca^{2+} is more likely to reach NOS-GCK complexes on secretory granules than extracellular Ca^{2+} because the vast majority of insulin granules are located in the cell interior away from the plasma membrane.

Dynamic Ca^{2+} Oscillations and GCK Activation—Both cytoplasmic Ca^{2+} and metabolism (60) are known to exhibit oscillatory behaviors, and connections between the two have been observed (61). Suggested mechanisms tying metabolic oscillations to Ca^{2+} oscillations most frequently invoke PFK2, although this is not without controversy (62). The dual oscillator theory was derived from computational muscle models and emphasizes PFK2 activity. Importantly, these models assume a permissive role for GCK and static activity (63). Although this assumption should hold true for tissues, such as skeletal muscle, that phosphorylate glucose using hexokinase, β cell metabolism has a much different relationship with glucose because of its dependence on GCK. As Fridlyland and Phillipson (64) point out, β cells are notable for the "near-dominant" control of glycolysis by GCK activity . Indeed, even in the dual oscillator model, a precise amount of GCK activity is needed for the simulations to work because oscillations disappear with too little or too much GCK activity (63). Future work is required to fully unravel the influence of dynamic GCK activity on metabolic and Ca^{2+} oscillations.

Mechanism of GCK Control by ER Ca^{2+} Channels—Our results also show sensitivity of GCK regulation to both IP_3R and ryanodine receptor regulation. This was not unexpected because both receptor systems couple strongly to the generation of IP_3 (15, 16). Even so, it is unclear how generalizable our findings are with regard to the specific receptors involved in ER Ca^{2+} release. Some studies clearly favor a role for IP_3Rs over ryanodine receptors in receptor-mediated potentiation of

secretion (65), although expression of ryanodine receptors in islets is indeed prevalent, and their high conductance for Ca^{2+} suggests a prominent role in β cell Ca^{2+}-induced Ca^{2+} release (66). Additional mechanisms for ER Ca^{2+} release have also been described, such as through nicotinic acid adenine dinucleotide phosphate (67). Even so, it is likely that individual mechanisms will prove to be synergistic, given the relationship between cytoplasmic Ca^{2+} concentration and GCK activation.

We favor an integrative model where islets respond to a variety of factors in the extracellular milieu, including glucose, gap-junctional communication, and hormonal and, likely, neuronal inputs to produce a coordinated and integral secretory output. Naturally, further investigation will be required to quantitatively assess the control strength of the various possible regulatory mechanisms over GCK activation. Our optimized FRET-GCK sensor is perhaps a useful tool for such an investigation.

Author Contributions—M. L. M. and K. M. S. performed the experiments and analyzed the data. M. A. R. conceived the experiments, assisted with data analysis, and wrote the manuscript.

References

1. Larion, M., Salinas, R. K., Bruschweiler-Li, L., Miller, B. G., and Brüschweiler, R. (2012) Order-disorder transitions govern kinetic cooperativity and allostery of monomeric human glucokinase. *PLoS Biol.* **10,** e1001452
2. Rizzo, M. A., and Piston, D. W. (2003) Regulation of β cell glucokinase by *S*-nitrosylation and association with nitric oxide synthase. *J. Cell Biol.* **161,** 243–248
3. Massa, L., Baltrusch, S., Okar, D. A., Lange, A. J., Lenzen, S., and Tiedge, M. (2004) Interaction of 6-phosphofructo-2-kinase/fructose-2,6-bisphosphatase (PFK-2/FBPase-2) with glucokinase activates glucose phosphorylation and glucose metabolism in insulin-producing cells. *Diabetes* **53,** 1020–1029
4. Baltrusch, S., Langer, S., Massa, L., Tiedge, M., and Lenzen, S. (2006) Improved metabolic stimulus for glucose-induced insulin secretion through GK and PFK-2/FBPase-2 coexpression in insulin-producing RINm5F cells. *Endocrinology* **147,** 5768–5776
5. Ding, S. Y., Tribble, N. D., Kraft, C. A., Markwardt, M., Gloyn, A. L., and Rizzo, M. A. (2010) Naturally occurring glucokinase mutations are associated with defects in posttranslational *S*-nitrosylation. *Mol. Endocrinol.* **24,** 171–177
6. Ding, S. Y., Nkobena, A., Kraft, C. A., Markwardt, M. L., and Rizzo, M. A. (2011) Glucagon-like peptide 1 stimulates post-translational activation of glucokinase in pancreatic β cells. *J. Biol. Chem.* **286,** 16768–16774
7. Markwardt, M. L., Nkobena, A., Ding, S. Y., and Rizzo, M. A. (2012) Association with nitric oxide synthase on insulin secretory granules regulates glucokinase protein levels. *Mol. Endocrinol.* **26,** 1617–1629
8. Rizzo, M. A., Magnuson, M. A., Drain, P. F., and Piston, D. W. (2002) A functional link between glucokinase binding to insulin granules and conformational alterations in response to glucose and insulin. *J. Biol. Chem.* **277,** 34168–34175
9. Hao, M., Head, W. S., Gunawardana, S. C., Hasty, A. H., and Piston, D. W. (2007) Direct effect of cholesterol on insulin secretion: a novel mechanism for pancreatic β-cell dysfunction. *Diabetes* **56,** 2328–2338
10. Abu-Soud, H. M., and Stuehr, D. J. (1993) Nitric oxide synthases reveal a role for calmodulin in controlling electron transfer. *Proc. Natl. Acad. Sci. U.S.A.* **90,** 10769–10772
11. Abu-Soud, H. M., Yoho, L. L., and Stuehr, D. J. (1994) Calmodulin controls neuronal nitric-oxide synthase by a dual mechanism: activation of intra- and interdomain electron transfer. *J. Biol. Chem.* **269,** 32047–32050
12. Panda, K., Ghosh, S., and Stuehr, D. J. (2001) Calmodulin activates intersubunit electron transfer in the neuronal nitric-oxide synthase dimer. *J. Biol. Chem.* **276,** 23349–23356
13. Nunemaker, C. S., Buerk, D. G., Zhang, M., and Satin, L. S. (2007) Glucose-induced release of nitric oxide from mouse pancreatic islets as detected with nitric oxide-selective glass microelectrodes. *Am. J. Physiol. Endocrinol. Metab.* **292,** E907–912
14. Bertram, R., Sherman, A., and Satin, L. (2010) Electrical bursting, calcium oscillations, and synchronization of pancreatic islets. *Adv. Exp. Med. Biol.* **654,** 261–279
15. White, M. F. (2006) Regulating insulin signaling and β-cell function through IRS proteins. *Can. J. Physiol. Pharmacol.* **84,** 725–737
16. Doyle, M. E., and Egan, J. M. (2007) Mechanisms of action of glucagon-like peptide 1 in the pancreas. *Pharmacol. Ther.* **113,** 546–593
17. Ni, Q., Ganesan, A., Aye-Han, N. N., Gao, X., Allen, M. D., Levchenko, A., and Zhang, J. (2011) Signaling diversity of PKA achieved via a Ca^{2+}-cAMP-PKA oscillatory circuit. *Nat. Chem. Biol.* **7,** 34–40
18. Haataja, L., Snapp, E., Wright, J., Liu, M., Hardy, A. B., Wheeler, M. B., Markwardt, M. L., Rizzo, M., and Arvan, P. (2013) Proinsulin intermolecular interactions during secretory trafficking in pancreatic β cells. *J. Biol. Chem.* **288,** 1896–1906
19. Markwardt, M. L., Kremers, G. J., Kraft, C. A., Ray, K., Cranfill, P. J., Wilson, K. A., Day, R. N., Wachter, R. M., Davidson, M. W., and Rizzo, M. A. (2011) An improved cerulean fluorescent protein with enhanced brightness and reduced reversible photoswitching. *PLoS ONE* **6,** e17896
20. Rizzo, M. A., Springer, G., Segawa, K., Zipfel, W. R., and Piston, D. W. (2006) Optimization of pairings and detection conditions for measurement of FRET between cyan and yellow fluorescent proteins. *Microsc. Microanal.* **12,** 238–254
21. Zhang, F., Wang, L. P., Brauner, M., Liewald, J. F., Kay, K., Watzke, N., Wood, P. G., Bamberg, E., Nagel, G., Gottschalk, A., and Deisseroth, K. (2007) Multimodal fast optical interrogation of neural circuitry. *Nature* **446,** 633–639
22. He, T. C., Zhou, S., da Costa, L. T., Yu, J., Kinzler, K. W., and Vogelstein, B. (1998) A simplified system for generating recombinant adenoviruses. *Proc. Natl. Acad. Sci. U.S.A.* **95,** 2509–2514
23. Wier, W. G., Rizzo, M. A., Raina, H., and Zacharia, J. (2008) A technique for simultaneous measurement of Ca^{2+}, FRET fluorescence and force in intact mouse small arteries. *J. Physiol.* **586,** 2437–2443
24. Rizzo, M. A., Springer, G. H., Granada, B., and Piston, D. W. (2004) An improved cyan fluorescent protein variant useful for FRET. *Nat. Biotechnol.* **22,** 445–449
25. Gloyn, A. L., Odili, S., Buettger, C., Njolstad, P. R., Shiota, C., Magnuson, M. A., and Matschinsky, F. M. (2004) in *Glucokinase and Glycemic Disease: From Basics to Novel Therapeutics* (Matschinsky, F. M., and Magnuson, M. A. eds.) pp. 92–109, Karger, Basel, Switzerland
26. Bennett, B. D., Jetton, T. L., Ying, G., Magnuson, M. A., and Piston, D. W. (1996) Quantitative subcellular imaging of glucose metabolism within intact pancreatic islets. *J. Biol. Chem.* **271,** 3647–3651
27. Maruyama, T., Kanaji, T., Nakade, S., Kanno, T., and Mikoshiba, K. (1997) 2APB, 2-aminoethoxydiphenyl borate, a membrane-penetrable modulator of Ins(1,4,5)P3-induced Ca^{2+} release. *J. Biochem.* **122,** 498–505
28. Meissner, G., Darling, E., and Eveleth, J. (1986) Kinetics of rapid Ca^{2+} release by sarcoplasmic reticulum: effects of Ca^{2+}, Mg^{2+}, and adenine nucleotides. *Biochemistry* **25,** 236–244
29. Lai, F. A., Anderson, K., Rousseau, E., Liu, Q. Y., and Meissner, G. (1988) Evidence for a Ca^{2+} channel within the ryanodine receptor complex from cardiac sarcoplasmic reticulum. *Biochem. Biophys. Res. Commun.* **151,** 441–449
30. Vangheluwe, P., Raeymaekers, L., Dode, L., and Wuytack, F. (2005) Modulating sarco(endo)plasmic reticulum Ca^{2+} ATPase 2 (SERCA2) activity: cell biological implications. *Cell Calcium* **38,** 291–302
31. Gromada, J., Dissing, S., Bokvist, K., Renström, E., Frøkjaer-Jensen, J., Wulff, B. S., and Rorsman, P. (1995) Glucagon-like peptide I increases cytoplasmic calcium in insulin-secreting β TC3-cells by enhancement of intracellular calcium mobilization. *Diabetes* **44,** 767–774
32. Holz, G. G., Leech, C. A., Heller, R. S., Castonguay, M., and Habener, J. F. (1999) cAMP-dependent mobilization of intracellular Ca^{2+} stores by activation of ryanodine receptors in pancreatic β-cells: a Ca^{2+} signaling system stimulated by the insulinotropic hormone glucagon-like peptide-

1-(7–37). *J. Biol. Chem.* **274,** 14147–14156
33. Aspinwall, C. A., Qian, W. J., Roper, M. G., Kulkarni, R. N., Kahn, C. R., and Kennedy, R. T. (2000) Roles of insulin receptor substrate-1, phosphatidylinositol 3-kinase, and release of intracellular Ca^{2+} stores in insulin-stimulated insulin secretion in β-cells. *J. Biol. Chem.* **275,** 22331–22338
34. Roper, M. G., Qian, W. J., Zhang, B. B., Kulkarni, R. N., Kahn, C. R., and Kennedy, R. T. (2002) Effect of the insulin mimetic L-783,281 on intracellular Ca^{2+} and insulin secretion from pancreatic β-cells. *Diabetes* **51,** S43–49
35. Dyachok, O., and Gylfe, E. (2004) Ca^{2+}-induced Ca^{2+} release via inositol 1,4,5-trisphosphate receptors is amplified by protein kinase A and triggers exocytosis in pancreatic β-cells. *J. Biol. Chem.* **279,** 45455–45461
36. Lemmens, R., Larsson, O., Berggren, P. O., and Islam, M. S. (2001) Ca^{2+}-induced Ca^{2+} release from the endoplasmic reticulum amplifies the Ca^{2+} signal mediated by activation of voltage-gated L-type Ca^{2+} channels in pancreatic β-cells. *J. Biol. Chem.* **276,** 9971–9977
37. Beauvois, M. C., Arredouani, A., Jonas, J. C., Rolland, J. F., Schuit, F., Henquin, J. C., and Gilon, P. (2004) Atypical Ca^{2+}-induced Ca^{2+} release from a sarco-endoplasmic reticulum Ca^{2+}-ATPase 3-dependent Ca^{2+} pool in mouse pancreatic β-cells. *J. Physiol.* **559,** 141–156
38. Park, J. H., Kim, S. J., Park, S. H., Son, D. G., Bae, J. H., Kim, H. K., Han, J., and Song, D. K. (2012) Glucagon-like peptide-1 enhances glucokinase activity in pancreatic β-cells through the association of Epac2 with Rim2 and Rab3A. *Endocrinology* **153,** 574–582
39. DiPilato, L. M., and Zhang, J. (2009) The role of membrane microdomains in shaping β2-adrenergic receptor-mediated cAMP dynamics. *Mol. Biosyst.* **5,** 832–837
40. Nakazaki, M., Ishihara, H., Kakei, M., Inukai, K., Asano, T., Miyazaki, J. I., Tanaka, H., Kikuchi, M., Yada, T., and Oka, Y. (1998) Repetitive mitochondrial Ca^{2+} signals synchronize with cytosolic Ca^{2+} oscillations in the pancreatic β-cell line, MIN6. *Diabetologia* **41,** 279–286
41. Calabrese, A., Zhang, M., Serre-Beinier, V., Caton, D., Mas, C., Satin, L. S., and Meda, P. (2003) Connexin 36 controls synchronization of Ca^{2+} oscillations and insulin secretion in MIN6 cells. *Diabetes* **52,** 417–424
42. Mehta, S., Aye-Han, N. N., Ganesan, A., Oldach, L., Gorshkov, K., and Zhang, J. (2014) Calmodulin-controlled spatial decoding of oscillatory Ca^{2+} signals by calcineurin. *eLife* **3,** e03765
43. Landa, L. R., Jr., Harbeck, M., Kaihara, K., Chepurny, O., Kitiphongspattana, K., Graf, O., Nikolaev, V. O., Lohse, M. J., Holz, G. G., and Roe, M. W. (2005) Interplay of Ca^{2+} and cAMP signaling in the insulin-secreting MIN6 β-cell line. *J. Biol. Chem.* **280,** 31294–31302
44. Nagel, G., Brauner, M., Liewald, J. F., Adeishvili, N., Bamberg, E., and Gottschalk, A. (2005) Light activation of channelrhodopsin-2 in excitable cells of *Caenorhabditis elegans* triggers rapid behavioral responses. *Curr. Biol.* **15,** 2279–2284
45. Lin, J. Y., Lin, M. Z., Steinbach, P., and Tsien, R. Y. (2009) Characterization of engineered channelrhodopsin variants with improved properties and kinetics. *Biophys. J.* **96,** 1803–1814
46. Palmer, A. E., Giacomello, M., Kortemme, T., Hires, S. A., Lev-Ram, V., Baker, D., and Tsien, R. Y. (2006) Ca^{2+} indicators based on computationally redesigned calmodulin-peptide pairs. *Chem. Biol.* **13,** 521–530
47. McMurry, J. L., Chrestensen, C. A., Scott, I. M., Lee, E. W., Rahn, A. M., Johansen, A. M., Forsberg, B. J., Harris, K. D., and Salerno, J. C. (2011) Rate, affinity and calcium dependence of nitric oxide synthase isoform binding to the primary physiological regulator calmodulin. *FEBS J* **278,** 4943–4954
48. Stuehr, D. J. (1999) Mammalian nitric oxide synthases. *Biochim. Biophys. Acta* **1411,** 217–230
49. Smedler, E., and Uhlén, P. (2014) Frequency decoding of calcium oscillations. *Biochim. Biophys. Acta* **1840,** 964–969
50. Stubbs, M., Aiston, S., and Agius, L. (2000) Subcellular localization, mobility, and kinetic activity of glucokinase in glucose-responsive insulin-secreting cells. *Diabetes* **49,** 2048–2055
51. Baltrusch, S., and Lenzen, S. (2007) Novel insights into the regulation of the bound and diffusible glucokinase in MIN6 β-cells. *Diabetes* **56,** 1305–1315
52. Putney, J. W. (2010) Pharmacology of store-operated calcium channels. *Mol. Interv.* **10,** 209–218
53. Zhu, S., Larkin, D., Lu, S., Inouye, C., Haataja, L., Anjum, A., Kennedy, R., Castle, D., and Arvan, P. (2015) Monitoring C-peptide storage and secretion in islet β cells *in vitro* and *in vivo*. *Diabetes* 10.2337/db15–1264
54. Rhodes, C. J., White, M. F., Leahy, J. L., and Kahn, S. E. (2013) Direct autocrine action of insulin on β-cells: does it make physiological sense? *Diabetes* **62,** 2157–2163
55. Sandoval, D. A., and D'Alessio, D. A. (2015) Physiology of proglucagon peptides: role of glucagon and GLP-1 in health and disease. *Physiol. Rev.* **95,** 513–548
56. Schwetz, T. A., Reissaus, C. A., and Piston, D. W. (2014) Differential stimulation of insulin secretion by GLP-1 and Kisspeptin-10. *PLoS ONE* **9,** e113020
57. Song, W. J., Mondal, P., Wolfe, A., Alonso, L. C., Stamateris, R., Ong, B. W., Lim, O. C., Yang, K. S., Radovick, S., Novaira, H. J., Farber, E. A., Farber, C. R., Turner, S. D., and Hussain, M. A. (2014) Glucagon regulates hepatic kisspeptin to impair insulin secretion. *Cell Metab.* **19,** 667–681
58. Fridlyand, L. E., Harbeck, M. C., Roe, M. W., and Philipson, L. H. (2007) Regulation of cAMP dynamics by Ca^{2+} and G protein-coupled receptors in the pancreatic β-cell: a computational approach. *Am. J. Physiol. Cell Physiol.* **293,** C1924–1933
59. Quesada, I., Martín, F., and Soria, B. (2000) Nutrient modulation of polarized and sustained submembrane Ca^{2+} microgradients in mouse pancreatic islet cells. *J. Physiol.* **525,** 159–167
60. Luciani, D. S., Misler, S., and Polonsky, K. S. (2006) Ca^{2+} controls slow NAD(P)H oscillations in glucose-stimulated mouse pancreatic islets. *J. Physiol.* **572,** 379–392
61. Merrins, M. J., Van Dyke, A. R., Mapp, A. K., Rizzo, M. A., and Satin, L. S. (2013) Direct measurements of oscillatory glycolysis in pancreatic islet β-cells using novel fluorescence resonance energy transfer (FRET) biosensors for pyruvate kinase M2 activity. *J. Biol. Chem.* **288,** 33312–33322
62. Diederichs, F. (2008) Metabolic fluxes and stoichiometry of glucose metabolism. *Biophys. J.* **94,** 5079; discussion 5080
63. Bertram, R., Sherman, A., and Satin, L. S. (2007) Metabolic and electrical oscillations: partners in controlling pulsatile insulin secretion. *Am. J. Physiol. Endocrinol. Metab.* **293,** E890–900
64. Fridlyand, L. E., and Phillipson, L. H. (2011) Mechanisms of glucose sensing in the pancreatic β-cell: a computational systems-based analysis. *Islets* **3,** 224–230
65. Dzhura, I., Chepurny, O. G., Kelley, G. G., Leech, C. A., Roe, M. W., Dzhura, E., Afshari, P., Malik, S., Rindler, M. J., Xu, X., Lu, Y., Smrcka, A. V., and Holz, G. G. (2010) Epac2-dependent mobilization of intracellular Ca^{2+} by glucagon-like peptide-1 receptor agonist exendin-4 is disrupted in β-cells of phospholipase C-ϵ knockout mice. *J. Physiol.* **588,** 4871–4889
66. Islam, M. (2002) The ryanodine receptor calcium channel of β-cells: molecular regulation and physiological significance. *Diabetes* **51,** 1299–1309
67. Johnson, J. D., and Misler, S. (2002) Nicotinic acid-adenine dinucleotide phosphate-sensitive calcium stores initiate insulin signaling in human β cells. *Proc. Natl. Acad. Sci. U.S.A.* **99,** 14566–14571

Regulation of Glucokinase by Intracellular Calcium Levels in Pancreatic β Cells

Michele L. Markwardt, Kendra M. Seckinger and Mark A. Rizzo

J. Biol. Chem. 2016, 291:3000-3009.
doi: 10.1074/jbc.M115.692160 originally published online December 23, 2015